International Journal of Heat and Mass Transfer 52 (2009) 3873–3878

Contents lists available at ScienceDirect

International Journal of Heat and Mass Transfer

journal homepage: www.elsevier.com/locate/ijhmt

Technical Note

# The nonsimilar laminar wall plume in a constant transverse magnetic field

Asterios Pantokratoras

*School of Engineering, Democritus University of Thrace, 67100 Xanthi, Greece*

ARTICLE INFO

*Article history:*
Received 4 October 2008
Accepted by 6 March 2009
Available online 8 April 2009

*Keywords:*
Magnetohydrodynamics
Wall plume
Nonsimilar

ABSTRACT

The flow of a laminar wall plume in a constant transverse magnetic field is considered. The results are obtained with the numerical solution of the governing equations and cover both small and large $\xi$ values and Prandtl numbers from 0.01 to 100. The similar wall plume has been investigated in the past but the nonsimilar has not been treated until now and it is solved here for the first time.



## 1. Introduction

Wall plume is the flow produced by a line thermal source situated at the leading edge of a vertical adiabatic plate. Magnetohydrodynamics (MHD) is the field of fluid mechanics that encompasses the phenomena arising when a magnetic field is applied to an electrically conducting fluid. Water, air at high temperatures, plasma and especially liquid metals (lithium, mercury, sodium) are electrically conducting fluids. Static magnetic fields are known to be suitable for damping mean flow and turbulent motion in an electrically conducting liquid and for that reason they are used in damping of liquid-metal jets and plumes formed in industry [3,15]. For example, in the continuous casting of large steel slabs a magnetic field is used to suppress motion within the mould. Sometimes the motion takes the form of a submerged jet which feeds the mould from above [4]. Another field where plumes are formed is thermonuclear fusion (see for example [7,9,12]. There magnetic forces are used to confine the hot plasma away from the reactor walls.

The similar solution of the classical wall plume without magnetic field obtained by Liburdy and Faeth [8] and Jaluria and Gebhart [6] is now well known. Gray [5] investigated the wall plume in a transverse magnetic field and found that similarity solution exists only when the strength of the magnetic fields changes along the plate with the relation $B \sim x^{-2/5}$. When the magnetic field is constant the problem does not accept a similarity solution and has not been solved until now. The scope of the present note is to present the nonsimilar solution of the wall plume in a constant transverse magnetic field. The problem resembles with the nonsimilar flow along a vertical, isothermal plate in a constant transverse magnetic field, treated by Sparrow and Cess [13]. Although the present theory is too idealized for direct application in the cases mentioned in the previous paragraph, it can be expected that the qualitative insights will be useful.

## 2. The mathematical model

Consider the plane plume flow along a vertical adiabatic plate with $u$ and $v$ denoting respectively the velocity components in the $x$ and $y$ direction, where $x$ is the coordinate along the plate and $y$ is the coordinate perpendicular to $x$. For steady, two-dimensional flow the boundary layer equations with constant fluid properties are

$$\text{continuity equation}: \quad \frac{\partial u}{\partial x}+\frac{\partial v}{\partial y}=0 \tag{1}$$

$$\text{Momentum equation}: \quad u\frac{\partial u}{\partial x}+v\frac{\partial u}{\partial y}=\nu\frac{\partial^2 u}{\partial y^2}+g\beta(T-T_\infty)-\frac{\sigma B^2}{\rho}u \tag{2}$$

$$\text{Energy equation}: \quad u\frac{\partial T}{\partial x}+v\frac{\partial T}{\partial y}=a\frac{\partial^2 T}{\partial y^2} \tag{3}$$

where $\nu$ is the fluid kinematic viscosity, $g$ is the gravity acceleration, $T$ is the fluid temperature, $\beta$ is the fluid expansion coefficient, $\sigma$ is the electrical conductivity, $\rho$ is the density, $B$ is the strength of the magnetic field and $\alpha$ is the fluid thermal diffusivity. The boundary conditions are:

$$\text{At } y=0: \quad u=0, \quad v=0, \quad \partial T/\partial y=0 \tag{4}$$

$$\text{As } y\to\infty \quad u=0, \quad T=T_\infty \tag{5}$$

The Eqs. (1)–(3) represent a two-dimensional parabolic problem. Such a flow has a predominant velocity in the stream wise coordinate which in our case is the direction along the plate. We solved these equations directly using the finite difference meth-

*E-mail address:* apantokr@civil.duth.gr

0017-9310/$ - see front matter © 2009 Elsevier Ltd. All rights reserved.
doi:10.1016/j.ijheatmasstransfer.2009.03.002

od of Patankar [11]. The solution procedure starts with a known distribution of velocity and temperature at the plume exit ($x = 0$) and marches along the plate. At each downstream position the discretized Eqs. (2) and (3) are solved using the tridiagonal matrix algorithm (TDMA). Subsequently the cross-stream velocities $v$ were obtained from the continuity equation. The forward step size $\Delta x$ increases in proportion to the width of the calculation domain and was 1% of the outer boundary. In order to obtain a complete form of both the temperature and velocity profile at the same cross section we used a nonuniform lateral grid. $\Delta y$ takes small values near the surface (many grid points near the surface) and increases along $y$. The lateral grid cells were 300. It is known that the boundary layer thickness changes along $x$. For that reason the calculation domain must always be at least equal or wider than the boundary layer thickness. In each case we tried to have a calculation domain wider than the real boundary layer thickness. This has been done by trial and error. If the calculation domain was thin the velocity and temperature profiles were truncated. In this case we used another wider calculation domain in order to capture the entire velocity and temperature profiles. The parabolic (space marching) solution procedure is described analytically in the textbook of Patankar [11] which "remains to this day a model of simplicity and clarity and one of the most coherent explications of the finite volume technique ever written" [1]. This solution method has been used extensively in the literature, and has been included in fluid mechanics and heat transfer textbooks (see page 364 in [2], page 271 in [14] and page 124 in [10].

## 3. Results and discussion

Liburdy and Faeth [8] solved the wall plume problem using the following quantities. The transformed transverse coordinate is

$$\eta = \frac{y}{x} Gr^{1/5} \tag{6}$$

The nondimensional velocity $f'$ and nondimensional temperature $\theta$ are

$$f' = \frac{ux}{v} Gr^{-2/5} \tag{7}$$

$$\theta = k(T - T_\infty)Q^{-1} Gr^{1/5} Pr \tag{8}$$

where $Gr$ is the Grashof number

$$Gr = g\beta Q x^3 / (k v^2 Pr) \tag{9}$$

$Q$ is the heat flux

$$Q = \rho c_p \int_0^\infty u(T - T_\infty) dy \tag{10}$$

$Pr$ is the Prandtl number

$$Pr = v/a \tag{11}$$

and $k$ and $c_p$ are the fluid thermal conductivity and the specific heat. It should be mentioned here that the present problem does not accept a similarity solution and therefore the flow characteristics change in the streamwise direction. We found that the quantity $\xi$

$$\xi = \frac{\sigma B^2}{\rho} \left( \frac{\rho c_p x^2}{g\beta Q} \right)^{2/5} v^{1/5} \tag{12}$$

is the suitable parameter which expresses the relative importance of the magnetic forces to buoyancy forces. When $\xi = 0$ we have the classical wall plume without magnetic field. The above parameter $\xi$ is equivalent to parameter $\xi$ used by Sparrow and Cess [13] for the flow along a vertical isothermal plate.

In Table 1 the maximum velocity $f'_{max}$ and the wall temperature $\theta(0)$ for different $Pr$ numbers and different values of $\xi$ parameter are shown. In the same table the corresponding results by Liburdy and Faeth [8] for $\xi = 0$ are included. The comparison between our results and those of Liburdy and Faeth [8] is satisfactory. The differences are below 3%.

**Table 1**
Maximum velocity $f'_{max}$ and wall temperature $\theta(0)$ for different $Pr$ numbers and different values of $\xi$ parameter.

| $\xi$ | $Pr = 0.01$ | | $Pr = 0.1$ | | $Pr = 1$ | | $Pr = 10$ | | $Pr = 100$ | |
|---|---|---|---|---|---|---|---|---|---|---|
| | $f'_{max}$ | $\theta(0)$ | $f'_{max}$ | $\theta(0)$ | $f'_{max}$ | $\Theta(0)$ | $f'_{max}$ | $\theta(0)$ | $f'_{max}$ | $\theta(0)$ |
| 0.0 | 0.6083 Liburdy& Faeth | 0.1258 Liburdy& Faeth | 0.7352 Liburdy& Faeth | 0.3165 Liburdy& Faeth | 0.7341 Liburdy& Faeth | 0.8340 Liburdy& Faeth | 0.6380 Liburdy& Faeth | 2.6065 Liburdy& Faeth | 0.4841 Liburdy& Faeth | 9.5698 Liburdy& Faeth |
| 0.0 | 0.5969 | 0.1302 | 0.7162 | 0.3282 | 0.7265 | 0.8546 | 0.6455 | 2.6368 | 0.4748 | 9.4577 |
| 1.0 | 0.1878 | 0.1747 | 0.3909 | 0.4067 | 0.5201 | 0.9853 | 0.5162 | 2.8864 | 0.4353 | 9.8164 |
| 2.0 | 0.1088 | 0.2182 | 0.2307 | 0.4762 | 0.3953 | 1.0852 | 0.4515 | 3.0647 | 0.4065 | 9.9756 |
| 3.0 | 0.0820 | 0.2475 | 0.1718 | 0.5318 | 0.3204 | 1.1826 | 0.4103 | 3.1734 | 0.3835 | 10.1023 |
| 4.0 | | | 0.1429 | 0.5877 | 0.2730 | 1.2724 | 0.3774 | 3.2660 | 0.3667 | 10.2122 |
| 5.0 | | | 0.1242 | 0.6374 | 0.2390 | 1.3486 | 0.3496 | 3.3598 | 0.3530 | 10.3628 |
| 6.0 | | | 0.1073 | 0.6594 | 0.2146 | 1.4214 | 0.3272 | 3.4453 | 0.3417 | 10.5041 |
| 7.0 | | | 0.0973 | 0.6981 | 0.1920 | 1.4607 | 0.3079 | 3.5310 | 0.3316 | 10.5778 |
| 8.0 | | | 0.0894 | 0.7300 | 0.1768 | 1.5234 | 0.2911 | 3.6177 | 0.3228 | 10.6505 |
| 9.0 | | | 0.0828 | 0.7559 | 0.1643 | 1.5798 | 0.2766 | 3.6977 | 0.3150 | 10.7512 |
| 10 | | | 0.0771 | 0.7838 | 0.1537 | 1.6360 | 0.2636 | 3.7774 | 0.3077 | 10.8504 |
| 15 | | | | | 0.1218 | 1.9268 | 0.2177 | 4.1866 | 0.2746 | 11.2102 |
| 20 | | | | | 0.1016 | 2.0972 | 0.1873 | 4.5073 | 0.2542 | 11.6012 |
| 25 | | | | | 0.0878 | 2.2446 | 0.1655 | 4.8034 | 0.2380 | 12.1004 |
| 30 | | | | | 0.0778 | 2.3860 | 0.1493 | 5.0577 | 0.2244 | 12.4113 |
| 40 | | | | | | | 0.1261 | 5.5257 | 0.2024 | 13.0456 |
| 50 | | | | | | | 0.1103 | 5.9409 | 0.1852 | 13.8294 |
| 60 | | | | | | | 0.0987 | 6.3062 | 0.1715 | 14.5218 |
| 70 | | | | | | | 0.0897 | 6.6230 | 0.1601 | 15.1522 |
| 80 | | | | | | | | | 0.1504 | 15.7403 |
| 90 | | | | | | | | | 0.1421 | 16.2879 |
| 100 | | | | | | | | | 0.1348 | 16.7881 |
| 110 | | | | | | | | | 0.1284 | 17.2568 |
| 120 | | | | | | | | | 0.1226 | 17.7072 |
| 130 | | | | | | | | | 0.1175 | 18.1284 |
| 140 | | | | | | | | | 0.1128 | 18.5385 |
| 150 | | | | | | | | | 0.1085 | 18.9170 |

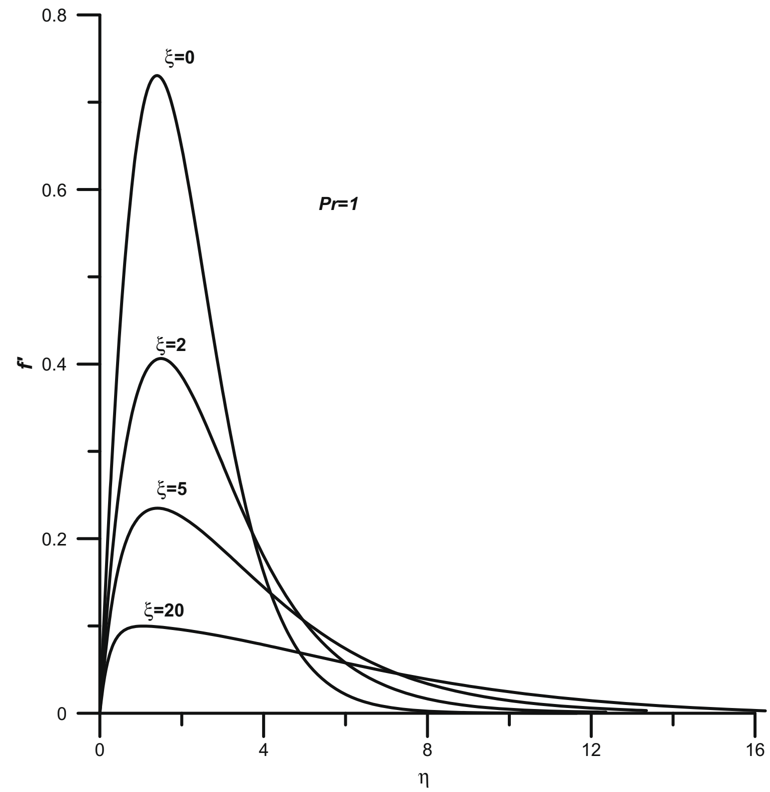


**Fig. 1.** Velocity profiles for different values of $\xi$ parameter and $Pr = 1$.

In Figs. 1 and 2 we present velocity and temperature profiles for $Pr = 1$ and different values of $\xi$ parameter while in Figs. 3 and 4 velocity and temperature profiles are shown for $\xi = 2$ and different $Pr$ numbers. It is seen that both velocity and temperature profiles

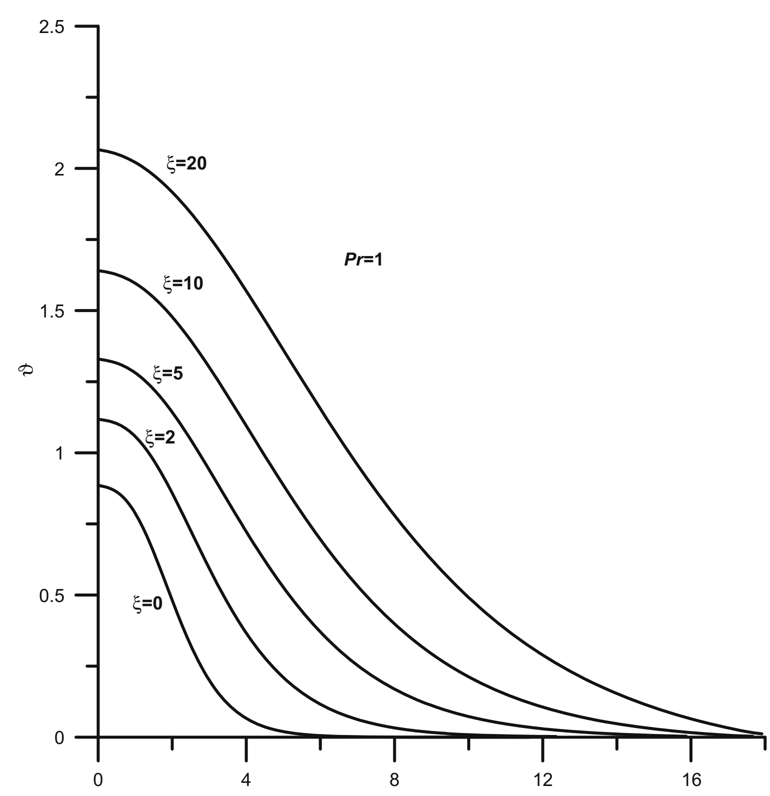


**Fig. 2.** Temperature profiles for different values of $\xi$ parameter and $Pr = 1$.

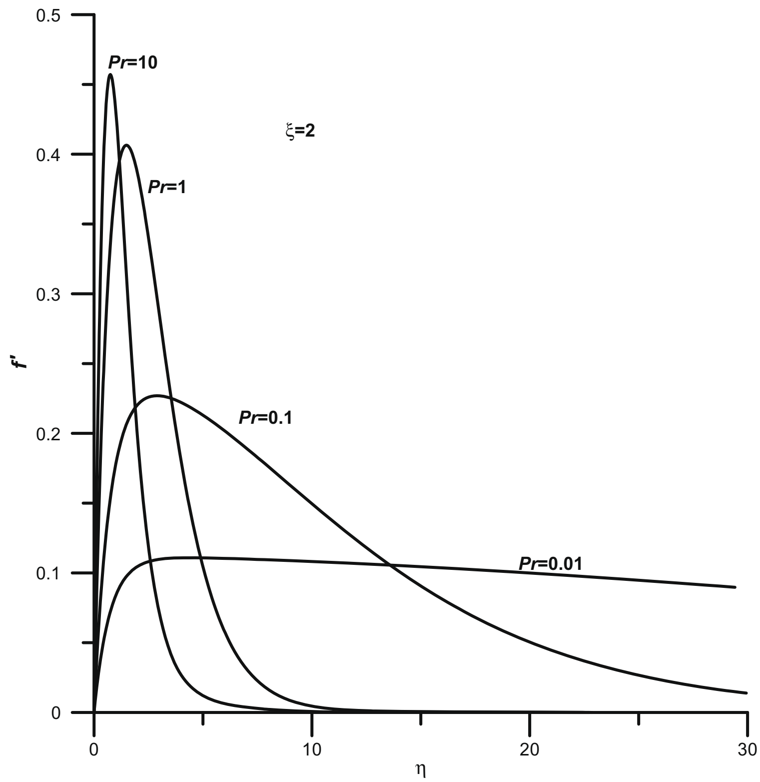


**Fig. 3.** Velocity profiles for $\xi = 2$ and different *Pr* numbers.

become thicker as $\xi$ increases, whereas velocity decreases and temperature increases with increasing $\xi$. The influence of *Pr* number on the results is the usual in boundary layer theory, that is, as *Pr* number increases both velocity and temperature profiles become thinner. From the above table and figures we see that as $\xi$ increases the magnetic field retards the flow and the flow tends to

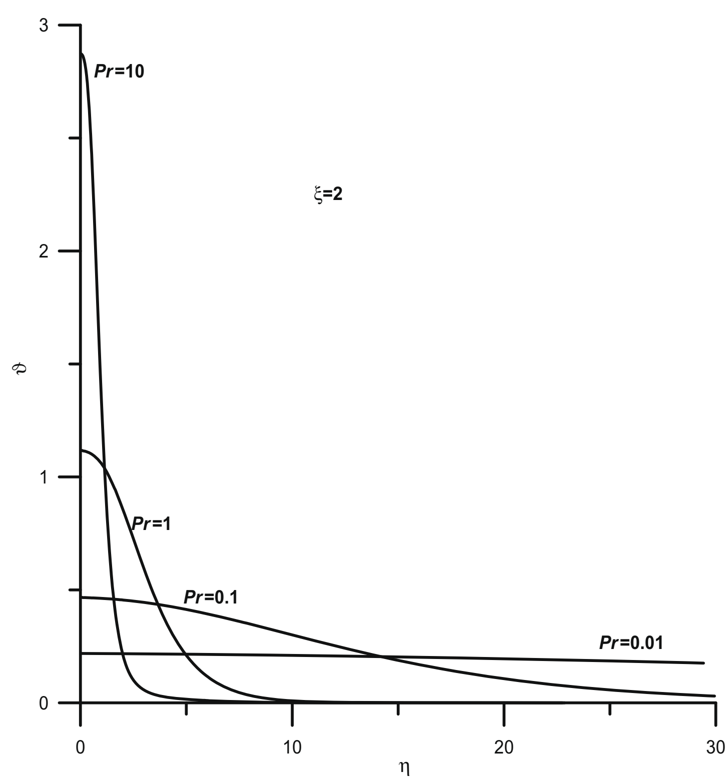


**Fig. 4.** Temperature profiles for $\xi = 2$ and different *Pr* numbers.

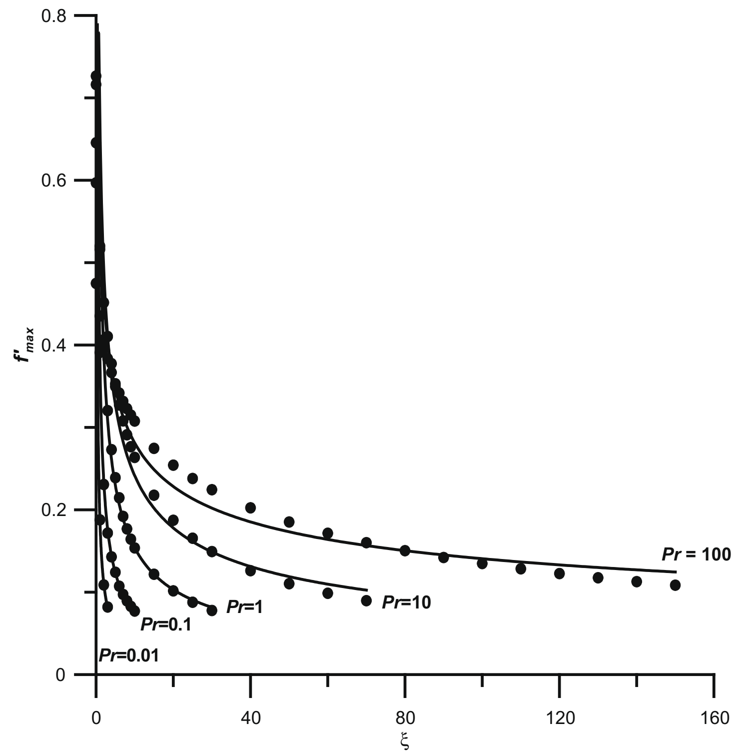


**Fig. 5.** Variation of dimensionless maximum velocity with $\xi$ for different Prandtl numbers.

disappear as $\xi$ increases. The results in the above table stop at approximately $\xi = 0.1$ where the plume velocity reaches a very small value. It is seen that the velocity decreases much faster as $Pr$ number decreases. The maximum velocity takes the value 0.1 at $\xi = 2$ for $Pr = 0.01$ while reaches the value 0.1 at $\xi = 150$ for $Pr = 100$.

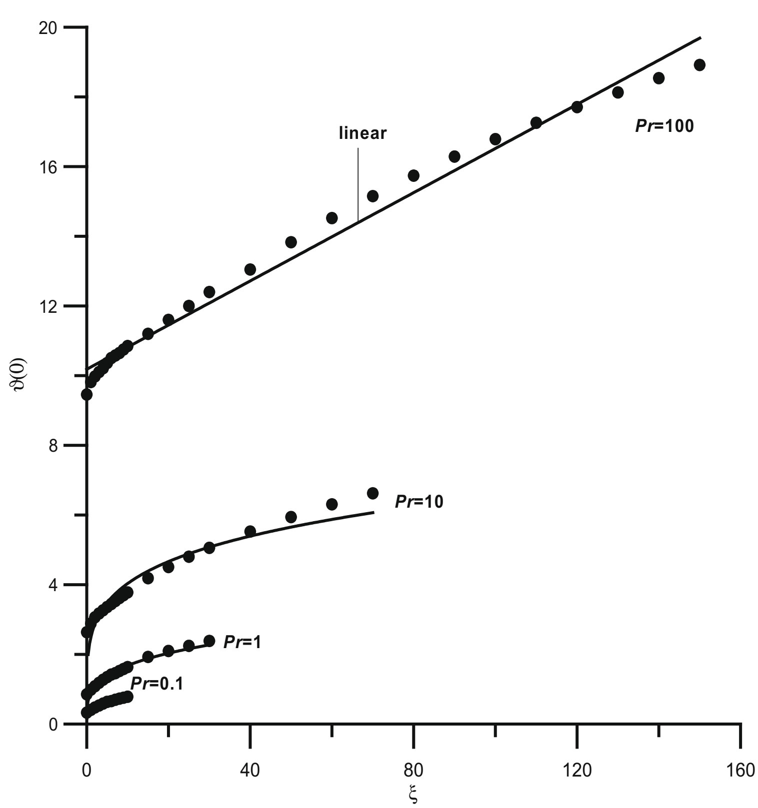


**Fig. 6.** Variation of dimensionless maximum temperature with $\xi$ for different Prandtl numbers.

In Figs. 5 and 6 the nondimensional maximum velocity and nondimensional maximum temperature are shown as functions of the nondimensional $\xi$ parameter. The best fit line for maximum velocity is power-law according to following relations

$$\ln(f'_{\max}) = -0.7579\ln(\xi) - 1.6779 \quad \text{for} \quad Pr = 0.01 \tag{13}$$

$$\ln(f'_{\max}) = -0.6989\ln(\xi) - 0.9674 \quad \text{for} \quad Pr = 0.1 \tag{14}$$

$$\ln(f'_{\max}) = -0.5774\ln(\xi) - 0.5422 \quad \text{for} \quad Pr = 1 \tag{15}$$

$$\ln(f'_{\max}) = -0.4402\ln(\xi) - 0.4072 \quad \text{for} \quad Pr = 10 \tag{16}$$

$$\ln(f'_{\max}) = -0.3008\ln(\xi) - 0.5760 \quad \text{for} \quad Pr = 100 \tag{17}$$

The corresponding relations for maximum temperature are

$$\ln(\theta(0)) = 0.3175\ln(\xi) - 1.7441 \quad \text{for} \quad Pr = 0.01 \tag{18}$$

$$\ln(\theta(0)) = 0.2913\ln(\xi) - 0.9269 \quad \text{for} \quad Pr = 0.1 \tag{19}$$

$$\ln(\theta(0)) = 0.2744\ln(\xi) - 0.1126 \quad \text{for} \quad Pr = 1 \tag{20}$$

$$\ln(\theta(0)) = 0.2098\ln(\xi) + 0.9114 \quad \text{for} \quad Pr = 10 \tag{21}$$

We see that for low $\xi$ values both $f'_{\max}$ and $\theta(0)$ follow the power-law but as $\xi$ increases these quantities tend to become linear and for that reason no best fit line can be used for $\theta(0)$ at $Pr = 100$.

## 4. Conclusions

In the present note the wall plume in a constant transverse magnetic field has been investigated numerically for the first time. The problem is nonsimilar and it is governed by a new parameter $\xi = \frac{\sigma B^2}{\rho}\left(\frac{\rho c_p x^2}{g\beta Q}\right)^{2/5} \nu^{1/5}$ which expresses the relative importance of the magnetic forces to buoyancy forces. As $\xi$ increases the magnetic field retards the flow and the nondimensional maximum velocity decreases whereas the nondimensional maximum temperature increases. The variation of the nondimensional maximum velocity and the nondimensional maximum temperature with $\xi$ follows approximately a power-law relation. The nondimensional maximum velocity and temperature increase with increasing Prandtl number. Both velocity and temperature profiles become thicker as $\xi$ increases and as Prandtl number increases both velocity and temperature profiles become thinner.

## References

[1] S. Acharya, J. Murthy, Foreword to the special issue on computational heat transfer, ASME J. Heat Transfer 129 (2007) 405–406.
[2] D. Anderson, J. Tannehill, R. Pletcher, Computational Fluid Mechanics and Heat Transfer, McGraw-Hiil Company, Mew York, 1984.
[3] P.A. Davidson, Magnetic damping of jets and vortices, J. Fluid Mech. 299 (1995) 153–186.
[4] P.A. Davidson, An Introduction to Magnetohydrodynamics, Cambridge University Press, Cambridge, 2006.
[5] D. Gray, The laminar wall plume in a transverse magnetic field, Int. J. Heat Mass Transfer 22 (1979) 1155–1158.
[6] Y. Jaluria, B. Gebhart, Buoyancy-induced flow arising from a line thermal source on an adiabatic vertical surface, Int. J. Heat Mass Transfer 20 (1977) 153–157.
[7] T.H. Kim, S.H. Nam, H.S. Park, J.K. Song, S.M. Park, Effects of transverse magnetic field on a laser-produced Zn plasma plume and ZnO films grown by pulsed laser deposition, Appl. Surf. Sci. 253 (2007) 8054–8058.
[8] J. Liburdy, G. Faeth, Theory of a steady laminar plume along a vertical adiabatic wall, Lett. Heat Mass Transfer 2 (1975) 407–418.
[9] S.H. Nam, M.J. Ko, M.A. Lee, H.S. Park, J.K. Song, S.M. Park, Effects of transverse magnetic field on laser-produced carbon plume in nitrogen atmosphere, Bull. Korean Chem. Soc. 28 (2007) 767–771.
[10] P. Oosthuizen, D. Naylor, Introduction to Convective Heat Transfer Analysis, McGraw-Hill, New York, 1999.
[11] S.V. Patankar, Numerical Heat Transfer and Fluid Flow, McGraw-Hill Book Company., New York, 1980.
[12] M.S. Rafique, M. Khaleeq-Ur-Rahmna, I. Riaz, R. Jalil, N. Farid, External magnetic field effect on plume images and X-ray emission from a nanosecond laser produced plasma, Laser and Particle Beams 26 (2008) 217–224.
[13] E.M. Sparrow, R.D. Cess, The effect of a magnetic field on free convection heat transfer, Int. J. Heat Mass Transfer 3 (1961) 267–274.
[14] F. White, Viscous Fluid Flow, third ed., McGraw-Hill, New York, 2006.
[15] C. Zhang, S. Eckert, G. Gerbeth, The flow structure of a bubble-driven liquid-metal jet in a horizontal magnetic field, J. Fluid Mech. 575 (2007) 57–82.